AFRL-RD-PS-
TN-2011-0043

PROPAGATION OF 3-D BEAMS USING A FINITE-DIFFERENCE ALGORITHM

Alan H. Paxton

Air Force Research Laboratory
3550 Aberdeen Ave SE
Kirtland AFB, NM 87117-577

22 May 2011

Interim Report

AIR FORCE RESEARCH LABORATORY
Directed Energy Directorate
3550 Aberdeen Ave SE
AIR FORCE MATERIEL COMMAND
KIRTLAND AIR FORCE BASE, NM 87117-5776

NOTICE AND SIGNATURE PAGE

Using Government drawings, specifications, or other data included in this document for any purpose other than Government procurement does not in any way obligate the U.S. Government. The fact that the Government formulated or supplied the drawings, specifications, or other data does not license the holder or any other person or corporation; or convey any rights or permission to manufacture, use, or sell any patented invention that may relate to them.

This report was cleared for public release by the Air Force Research Laboratory [insert TD site] Public Affairs Office and is available to the general public, including foreign nationals. Copies may be obtained from the Defense Technical Information Center (DTIC) (http://www.dtic.mil).

AFRL-RD-PS-TN-2011-0043 HAS BEEN REVIEWED AND IS APPROVED FOR PUBLICATION IN ACCORDANCE WITH ASSIGNED DISTRIBUTION STATEMENT.

//Signed//	//Signed//
ALAN H. PAXTON, DR-III	MICHAEL F. SHEEHAN, DR-III, DAF
Project Manager	Acting Chief, Laser Division

This report is published in the interest of scientific and technical information exchange, and its publication does not constitute the Government's approval or disapproval of its ideas or findings.

REPORT DOCUMENTATION PAGE

Form Approved
OMB No. 0704-0188

1. REPORT DATE *(DD-MM-YYYY)*	2. REPORT TYPE	3. DATES COVERED *(From - To)*
05-22-11	Interim Report	1 November 2004-22 May 2011

4. TITLE AND SUBTITLE

Propagation of 3-D Beams Using A Finite-Difference Algorithm

5a. CONTRACT NUMBER
In-House

5b. GRANT NUMBER

5c. PROGRAM ELEMENT NUMBER
603605/602605

6. AUTHOR(S)

Alan Paxton

5d. PROJECT NUMBER

5e. TASK NUMBER

5f. WORK UNIT NUMBER
DF297840

7. PERFORMING ORGANIZATION NAME(S) AND ADDRESS(ES)

Air Force Research Laboratory
3550 Aberdeen Avenue SE
Kirtland AFB, NM 87117-5776

8. PERFORMING ORGANIZATION REPORT NUMBER

9. SPONSORING / MONITORING AGENCY NAME(S) AND ADDRESS(ES)
Air Force Research Laboratory
3550 Aberdeen Ave SE
Kirtland AFB, NM 87117-5776

10. SPONSOR/MONITOR'S ACRONYM(S)
AFRL/RDLA

11. SPONSOR/MONITOR'S REPORT NUMBER(S)
AFRL-RD-PS-TN-2011-0043

12. DISTRIBUTION / AVAILABILITY STATEMENT
Approved for Public Release; Distribution Unlimited. "Government Purpose Rights."

13. SUPPLEMENTARY NOTES
Proceedings of SPIE Vol. 7579; 2010. 377ABW-2010-0072 20 Jan 2010

14. ABSTRACT

We discuss practical aspects of the use of the finite-difference, alternating-direction implicit (ADI), numerical solution of the paraxial wave equation, for the free-space propagation of light beams. Results of calculations solving the finite-difference equations are compared with fresnal-integral solutions. Calculations are for round beams, but the field is represented in cartesian coordinates. Modes for empty unstable resonators are also obtained using the finite-difference algorithm and are compared with fresnal- difference.

15. SUBJECT TERMS
Beam propagation; wave optics; paraxial wave equation; finite difference

16. SECURITY CLASSIFICATION OF:			17. LIMITATION OF ABSTRACT	18. NUMBER OF PAGES	19a. NAME OF RESPONSIBLE PERSON
a. REPORT	b. ABSTRACT	c. THIS PAGE			Alan H. Paxton
Unclassified	Unclassified	Unclassified	SAR	12	19b. TELEPHONE NUMBER *(include area code)*

Propagation of 3-D Beams Using a Finite-Difference Algorithm: Practical Considerations

Alan H. Paxton

Air Force Research Laboratory, Directed Energy Directorate,
Kirtland Air Force Base, NM 87117-5776

Abstract

We discuss practical aspects of the use of the finite-difference, alternating-direction implicit (ADI), numerical solution of the paraxial wave equation, for the free-space propagation of light beams. Results of calculations solving the finite-difference equations are compared with fresnel-integral solutions. Calculations are for round beams, but the field is represented in cartesian coordinates. Modes for empty unstable resonators are also obtained using the finite-difference algorithm and are compared with fresnel-integral solutions.

Keywords: beam propagation; wave optics; paraxial wave equation; finite difference

1. INTRODUCTION

A finite-difference method may be useful for beam propagation in the numerical simulation of lasers. The representation of the field at many planes along the resonator axis, in the gain medium, may be necessary due to temperature variation, stress-induced birefringence, or dependence of the refractive index on the light intensity. A finite-difference algorithm can be computationally efficient for such cases. For 3-D propagation in cartesian coordinates, the alternating-direction-implicit method is unconditionally stable (for empty-space propagation). The values for the field at the next plane are obtained by solving a tri-diagonal matrix equation for each row and column of the field grid. The application of boundary conditions at the edges of the x, y grid is a consideration, where z is the propagation direction. We use a zero-field boundary condition with apodization of the field in the vicinity of the boundary. For the symmetrical test cases shown below, we could have used the boundary conditions for the complex field amplitude

$$\frac{\partial u}{\partial x} = 0 \quad \text{along the line} \quad x = 0 \tag{1}$$

$$\frac{\partial u}{\partial y} = 0 \quad \text{along the line} \quad y = 0 \tag{2}$$

Instead, the entire field array was included on the grid because the code was written to solve nonsymmetrical problems.

Cartesian coordinates are often preferable to cylindrical coordinates, even for treating round beams. All of the cells of the grid have the same dimensions, so wavefront aberrations of the same scale can be treated at any location in the beam. Moreover, round beams do not usually have cylindrical symmetry in high-average-power non-fiber lasers. The symmetry is broken due to misalignment of optical elements, flow in gas lasers, or the cooling geometries of solid-state lasers.

Rensch used finite-difference propagation in a simulation of a CO_2 laser.[1] More recent work on 3-D, finite-difference optical propagation, including non-paraxial methods, was reviewed and augmented by Bekker.[2]

2. FINITE DIFFERENCE APPROXIMATION TO THE PARAXIAL WAVE EQUATION

The paraxial wave equation can be written

$$\nabla_t^2 u - 2ik\frac{\partial u}{\partial z} = 0 \tag{3}$$

The problem is posed as an initial-value problem,[3] with the z spatial coordinate replacing the time coordinate of problems for which "initial-value" is taken literally. Applying the ADI method to this equation, two half-steps are applied successively. The first half-step is implicit in x and the second half-step is implicit in y.

$$\frac{-i\sigma}{2}[(u^{i+1/2}_{j-1,k} - 2u^{i+1/2}_{j,k} + u^{i+1/2}_{j+1,k}) + (u^{i}_{j,k-1} - 2u^{i}_{j,k} + u^{i}_{j,k+1})] - u^{i+1/2}_{j,k} + u^{i}_{j,k} = 0 \tag{4}$$

where

$$\sigma = \frac{\Delta z}{2k(\Delta s)^2} \text{ and } \Delta s = \Delta x = \Delta y \tag{5}$$

Index i corresponds to the z coordinate, j corresponds to x , and k corresponds to y. The second half-step is taken,

$$\frac{-i\sigma}{2}[(u^{i+1/2}_{j-1,k} - 2u^{i+1/2}_{j,k} + u^{i+1/2}_{j+1,k}) + (u^{i+1}_{j,k-1} - 2u^{i+1}_{j,k} + u^{i+1}_{j,k+1})] - u^{i+1}_{j,k} + u^{i+1/2}_{j,k} = 0 \tag{6}$$

More compact notation is sometimes used

$$\frac{-i\sigma}{2}(\delta^2_x u^{i+1/2} + \delta^2_y u^{i}) - u^{i+1/2} + u^{i} = 0 \tag{7}$$

$$\frac{-i\sigma}{2}(\delta^2_y u^{i+1} + \delta^2_x u^{i+1/2}) - u^{i+1} + u^{i+1/2} = 0 \tag{8}$$

Each half-step requires the solution of a tri-diagonal matrix equation for each row or column of the field array. For the results presented here, we set the complex field amplitude u to zero on the boundary. The matrix equation for the first half-step is,

$$\begin{pmatrix} B & A & & & & & & & & \\ A & B & A & & & & & & & \\ & A & B & A & & & & & & \\ & & & \cdot & & & & & & \\ & & & & \cdot & & & & & \\ & & & & & \cdot & & & & \\ & & & & & A & B & A & & \\ & & & & & & A & B & A & \\ & & & & & & & & A & B \end{pmatrix} \begin{pmatrix} u^{i+1/2}_{1,k} \\ u^{i+1/2}_{2,k} \\ u^{i+1/2}_{3,k} \\ \cdot \\ \cdot \\ \cdot \\ u^{i+1/2}_{m-2,k} \\ u^{i+1/2}_{m-1,k} \\ u^{i+1/2}_{m,k} \end{pmatrix} = \begin{pmatrix} R_1 \\ R_2 \\ R_3 \\ \cdot \\ \cdot \\ \cdot \\ R_{m-2} \\ R_{m-1} \\ R_m \end{pmatrix} \tag{9}$$

where $A = -1$; $B = 2(i/\sigma + 1)$; $R_i = u^i_{j,k-1} + 2(i/\sigma - 1)u^i_{j,k} + u^i_{j,k+1}$, and the transverse field grid has m by m points. For all i, j, and k, we set: $u^i_{0,k} = 0$; $u^i_{j,0} = 0$; $u^i_{m+1,k} = 0$; $u^i_{j,m+1} = 0$. The accuracy depends on the value of σ, with numerical error occurring for large values of σ.

The boundary condition would cause reflection of optical flux arriving at the edge of the grid. To prevent this, a smoothed aperture was included. The complex amplitude was clipped by a slightly apodized circular aperture after each half-step propagation. The complex amplitude was multiplied by a cosine window function with a width of 5 points. The aperture was located so that the cosine window was barely inside the grid at its closest points. For the calculated results presented here, the calculational grid was square, of width twice the initial diameter of the circular beam.

3. COMPARISON OF SOLUTIONS FOR PROPAGATION OF TOP-HAT BEAMS

We compare finite-difference solutions, for propagation of a beam, with fresnel-integral solutions. The fresnel integral was solved using a kernel averaged algorithm developed by Dwight Phelps.[4,5] A beam with uniform intensity and planar wave fronts passes through an initial circular aperture, the radius of which is 1. The aperture edge is usually slightly apodized. The beam with a slightly smoothed, top hat distribution propagates to a final

plane corresponding to a given fresnel number. Abrupt aperture edges would create field variation for which the transverse laplacian could not be represented by the difference equations, so smoothing of the field over several points might be required at the initial beam aperture. For the propagation of an apodized top-hat beam, unless the smoothing distance is smaller than or comparable to the outer fresnel-zone width, d, the apodization will affect the solution. The width is given by

$$d/a = 1 - \left(\frac{n-1}{n}\right)^{1/2}$$

where a is the aperture radius and n is the fresnel number. For $n = 5$, $d/a = 0.106$ and for $n = 10$, $d/a = 0.051$. The curves shown in Figs. 1 through 6 correspond to $n = 5$.

Before comparing finite-difference solutions with fresnel-integral solutions, we look at the effect of apodization of the aperture edge for the fresnel-integral solutions. The field is represented on a square grid with 256 by 256 points. The guard ratio is $r_g = 1.1$. That is, the grid width is 1.1 times the width of the initial aperture. The Phelps algorithm does not suffer from aliasing. The number of points over which the field is smoothed at the aperture edge, by a cosine window, varies for the plots in Fig. 1. The number of points is: Curve 1, $n_w = 0$; Curve 2, $n_w = 5$; Curve 3, $n_w = 10$; Curve 4, $n_w = 15$. The first three curves are very similar to each other, and the fourth is noticeably smoother. The outer fresnel zone has a width corresponding to 25 points. For all of the fresnel-integral results shown here, a grid of 256 by 256 points is used, and $r_g = 1.1$ except as otherwise noted.

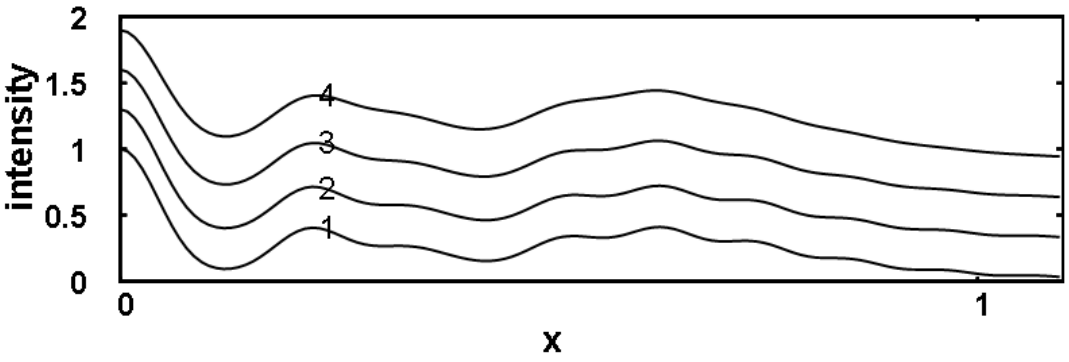

Figure 1. Calculated intensity for the propagation of a beam with uniform intensity, that has passed through a round aperture. The fresnel number is 5. The kernel averaged fresnel-integral algorithm was used. The beam was smoothed with a cosine window over n_w points. For Curve 1, $n_w = 0$; for Curve 2, $n_w = 5$; for Curve 3, $n_w = 10$; for Curve 4, $n_w = 15$.

Curves shown in Fig. 2 compare intensity plots for a fresnel-integral solution (solid) and for the finite-difference solution (dashed) for $n_w = 5$. For the finite-difference soultion, $r_g = 2.0$ and the grid was 466 by 466 points, so that the same number of points were inside the initial aperture for both calculations. The plots are very similar, with minor differences in the small-scale structure. The physical problem is not exactly the same for the two solutions. The fresnel integral corresponds to a field propagating through unobstructed space, whereas the finite-difference includes a cylindrical absorbing wall with twice the initial diameter of the beam.

Because the grid doesn't match the symmetry of the optical beam, it is worth checking how well the cylindrical symmetry of the initial aperture is preserved after propagation using the finite-difference algorithm. For the finite-difference calculation of Fig. 2, the intensity was evaluated by interpolation, along radial lines at angles, with the x-axis, of 0, $\pi/12$, $\pi/6$, and $\pi/4$. The four curves, shown in Fig. 3, are almost identical.

Curves shown in Fig. 4 are intensity plots for a fresnel-integral solution (solid), with $n_w = 10$, and for a finite-difference solution (dashed). For the finite-difference soultion, the grid was 232 by 232 points, half as many

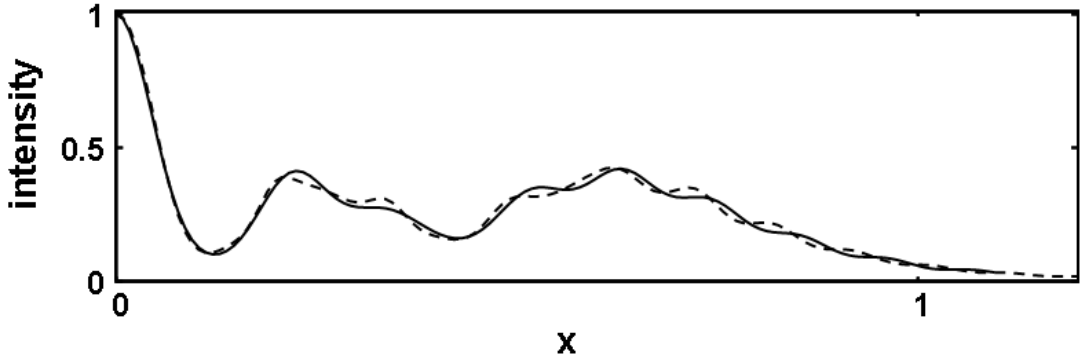

Figure 2. Intensity calculated with the fresnel-integral algorithm, solid line, and the intensity calculated with the finite-difference algorithm, dashed line. The aperture contained the same number of transverse points for each of the two algorithms, and the fresnel number was 5.

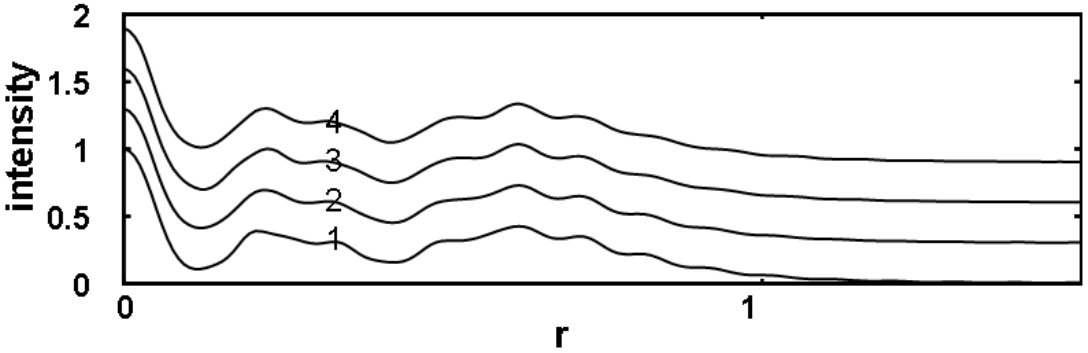

Figure 3. Field calculated with the finite-difference algorithm, for a fresnel number of 5. Traces of the intensity, evaluated by interpolation, are shown for angles, with the x-axis, of 0 Rad (Curve 1), $\pi/12$ Rad, $\pi/6$ Rad, and $\pi/4$ Rad (Curve 4).

in each dimension as for Fig. 2, The initial aperture was smoothed over $n_w = 5$ points, so that d/a would be the same for the two curves. The plots are not as close to each other as for Fig. 2.

Figure 5 shows plots of the intensity for a grid with 232 by 232 points. As for Fig. 3, the intensity was evaluated by interpolation, along radial lines at angles ,with the x-axis, of 0, $\pi/12$, $\pi/6$, and $\pi/4$. Unlike Fig. 3, these plots are noticeably different.

In Fig. 6, calculations with different numbers of grid points along z are compared. As Δz becomes larger than a certain value, we expect significant error to occur. We represent Δz in terms of the dimensionless variable σ. Values of σ are 1 ,2 ,4, and 8 for curves 1 through 4, respectively. The curve for $\sigma = 8$ is quite different from the others.

Plots for a fresnel number of 10 are shown in Fig. 7. The pairs of curves show the intensity calculated with the fresnel-integral algorithm, solid line, and the intensity calculated with the finite-difference algorithm, dashed line. The finite-difference (FD) solution on the bottom has a resolution of 466 by 466 grid points. The corresponding curve of the upper pair has a resolution of 932 by 932 points. For the bottom pair, $n_w = 5$, and for the upper FD solution, $n_w = 10$. The curve with higher resolution is in substantially better agreement with the fresnel-integral solution.

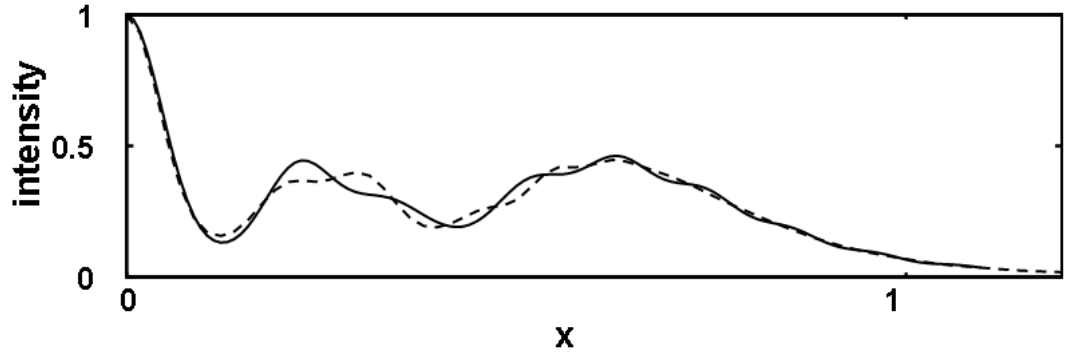

Figure 4. Intensity calculated with the fresnel-integral algorithm, solid line, and the intensity calculated with the finite-difference algorithm, dashed line. The transverse resolution for the finite-difference calculation was half as great as for Fig. 2.

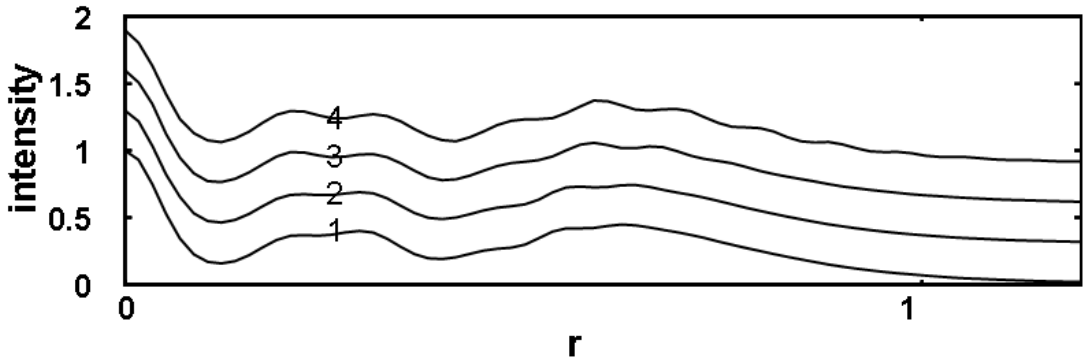

Figure 5. Field calculated with the finite-difference algorithm, for a fresnel number of 5. Traces of the intensity, evaluated by interpolation, are shown for angles, with the x-axis, of 0 Rad (Curve 1), $\pi/12$ Rad, $\pi/6$ Rad, and $\pi/4$ Rad (Curve 4). The transverse resolution for the finite-difference calculation was half as great as for Fig. 3.

4. COMPARISON OF UNSTABLE RESONATOR MODES

As final examples, we calculate the empty cavity modes for unstable resonators. The examples are for resonators with magnification of 2. Equivalent collimated propagation[6,7] was applied for the entire round trip (from the outcoupling plane back to the same plane) for the finite-difference calculation, and interpolation was used to magnify the beam. The fresnel-integral (FI) solution was for a confocal unstable resonator with a back mirror that filled the grid whose width was 1.2 times the geometric beam width. Equivalent collimated propagation was applied for each of the two propagation steps, and interpolation was also used for this case, to magnify the beam. For both examples: $n_w = 5$, the FI grid had 256 by 256 points, and the FD grid had 466 by 466 points.

Plots of the intensity for an unstable resonator with an equivalent fresnel number of 2.3 are shown in Fig. 8. The solid line corresponds to the fresnel-integral algorithm, and the dashed line resulted from the finite-difference algorithm. For this case, agreement is rather good, although the curves differ significantly near the resonator axis. The magnitudes calculated for the eigenvalue were 0.616 and 0.625, respectively.

Plots of the intensity for an unstable resonator with an equivalent fresnel number of 4.3 are shown in Fig. 9. The solid line corresponds to the fresnel-integral algorithm, and the dashed line resulted from the finite-difference algorithm. The FD grid had 466 by 466 points. Agreement is not good. The transverse resolution is apparently inadequate to resolve the field variation for this case.

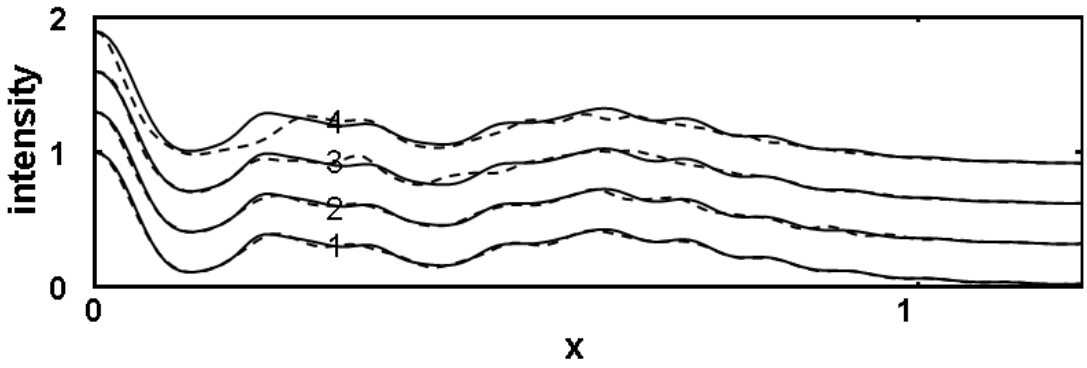

Figure 6. Field calculated with the finite-difference algorithm, for a fresnel number of 5. The solid curves are for $\sigma = 0.49$. The dashed traces are for varous values of σ: $\sigma = 1.0$, Curve 1; $\sigma = 2.0$, Curve2; $\sigma = 4.0$, Curve 3; and $\sigma = 8.0$, Curve 4. The transverse grid had 466 by 466 points.

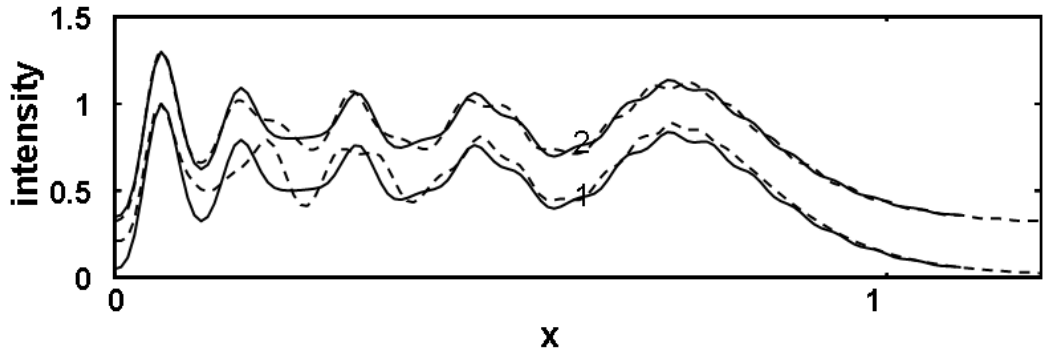

Figure 7. Intensity calculated with the fresnel-integral algorithm, solid line, and the intensity calculated with the finite-difference algorithm, dashed line. The finite-difference solution on the bottom has a resolution of 466 by 466 grid points. The corresponding curve of the upper pair has a resolution of 932 by 932 points. The fresnel number was 10.

5. CONCLUDING REMARKS

The effects of aperture diffraction can be treated adequately using the alternating-direction implicit finite-difference algorithm, although transverse resolution requirements are rather high. For the cases considered here, the approximate requirement for resolution in the z-direction is given by $\sigma \leq 4$. Unstable resonator modes can also be obtained using the finite-difference algorithm, if the problem is adequately resolved by the number of transverse grid points.

Fresnel-integral solutions are only valid if ϕ is a small angle,

$$\phi = \tan^{-1} \frac{2a}{l} \tag{10}$$

where l is the propagation distance. If this condition is not met, finite-difference solutions can not be validated by comparison with them. For propagation distances much shorter than this, geometrical optics, with some spill over at the beam edges, provides a reasonable approximation.

It is useful to understand the parameter values needed to treat aperture diffraction. The simulation of lasers usually involves compromise for the sake of practicality, however. As was observed by Anan'ev,[8] in lasers

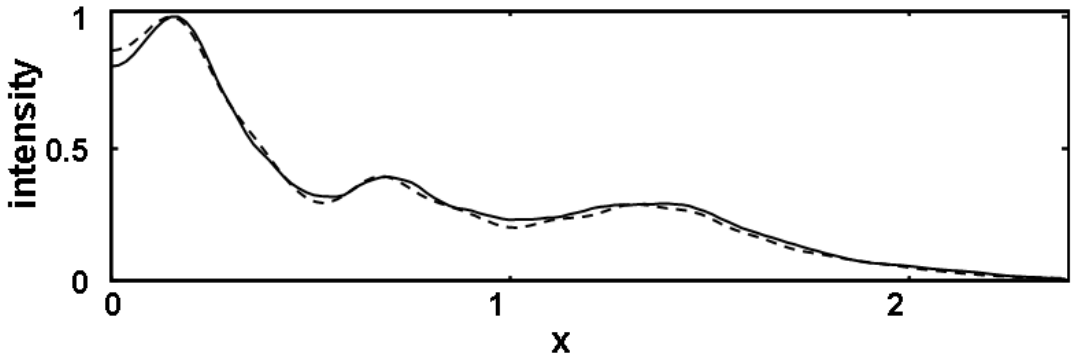

Figure 8. Intensity for unstable resonator calculated with the fresnel-integral algorithm, solid line, and the intensity calculated with the finite-difference algorithm, dashed line. The equivalent fresnel number was 2.3, and the resolution for the finite-difference solution was 466 by 466 points. The intensity is shown for the field incident on the outcoupling mirror. The edge of the outcoupling mirror is at x=1.

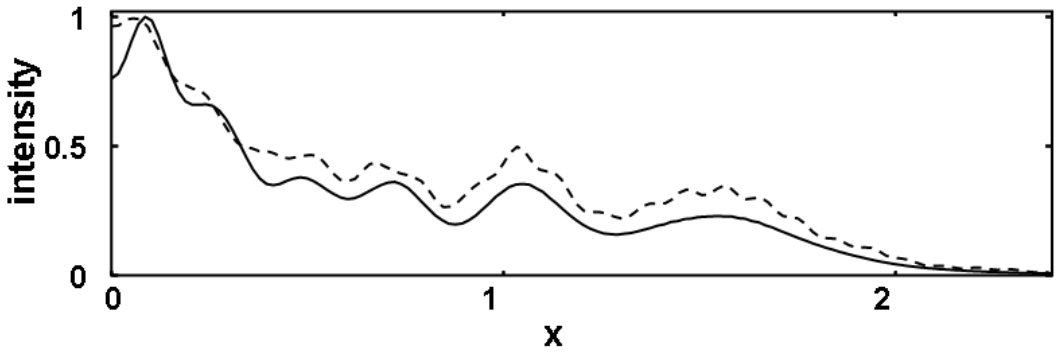

Figure 9. Intensity for unstable resonator calculated with the fresnel-integral algorithm, solid line, and the intensity calculated with the finite-difference algorithm, dashed line. The intensity is shown for the field incident on the outcoupling mirror. The equivalent fresnel number was 4.3, and the resolution for the finite-difference solution was 466 by 466 points.

with large outcoupling, which is usually the case if unstable resonators are used, the beam shape is determined mostly by the gain distribution rather than by diffraction. Precise treatment of aperture diffraction may play a secondary role, whereas the wave-optics treatment of strong aberrations may be quite significant in determining the laser beam quality. It is probably acceptable to use a finite-difference propagation algorithm, with a number of transverse grid points that would be inadequate for the calculation of bare cavity modes, to predict the power and beam quality of a laser with an unstable resonator. Often, the gain medium is separated by a considerable distance from one or both resonator end mirrors. Then it would be efficient to combine fresnel-integral propagation for empty regions with finite-difference propagation in regions with strong aberrations or nonlinear behavior.

6. ACKNOWLEDGMENT

This work was supported by the Department of Defense's High Energy Laser Joint Technology Office.

REFERENCES

[1] Rensch, D., "Three-dimensional unstable resonator calculations with laser medium," *Applied Optics* **13**(11), 2546–2561 (1974).

[2] Bekker, E. V., et al., "Wide-angle alternating-direction implicit finite-difference beam propagation method," *J. Lightwave Technology* **27**(14), 1874–1889 (2009).

[3] Richtmyer, R. D. and Morton, K. W., [*Difference Methods for Initial-Value Problems*], Wiley Interscience (1967).

[4] Dwight Phelps, Unpublished, "A new laser propagation algorithm using the fast fourier transform," Tech. Rep. AFWL-TR-74-344, pp 80-83 (1974).

[5] Milonni, P. W. and Paxton, A. H., "Model for unstable-resonator carbon monoxide electric-discharge laser," *J. Appl. Phys.* **49**(3), 1012–1027 (1978).

[6] Sziklas, E. A. and Siegman, A. E., "Mode calculations in unstable resonators with flowing saturable gain .2. fast fourier-transform method," *Applied Optics* **14**(8), 1874–1889 (1975).

[7] Siegman, A. E., [*Lasers*], University Science Books (1986).

[8] Anan'ev, Y. A., [*Laser Resonators and the Beam Divergence Problem*], Taylor & Francis (1992).

DISTRIBUTION LIST

DTIC/OCP
8725 John J. Kingman Rd, Suite 0944
Ft Belvoir, VA 22060-6218 1 cy

AFRL/RVIL
Kirtland AFB, NM 87117-5776 1 cy

Alan Paxton
Official Record Copy
AFRL/RDLA 1 cy